AIIM

Association for Information and Image Management

1100 Wayne Avenue, Suite 1100
Silver Spring, Maryland 20910

301/587-8202

Centimeter

1 2 3 4 5 6 7 8 9 10 11 12 13 14 15 mm

1 2 3 4 5

Inches

1.0 1.1 1.25 1.4 1.6 1.8 2.0 2.2 2.5 2.8 3.2 3.6 4.0 4.5 5.0 5.6 6.3

MANUFACTURED TO AIIM STANDARDS
BY APPLIED IMAGE, INC.

1 of 1

5/1 7-13-93 JS(2)

PREPARED FOR THE U.S. DEPARTMENT OF ENERGY,
UNDER CONTRACT DE-AC02-76-CHO-3073

PPPL-2917
UC-426

PPPL-2917

ION CYCLOTRON RANGE OF FREQUENCY HEATING ON THE TOKAMAK FUSION TEST REACTOR

BY

G. TAYLOR, M.G. BELL, H. BIGLARI, ET AL.

JUNE, 1993

PPPL PRINCETON PLASMA PHYSICS LABORATORY

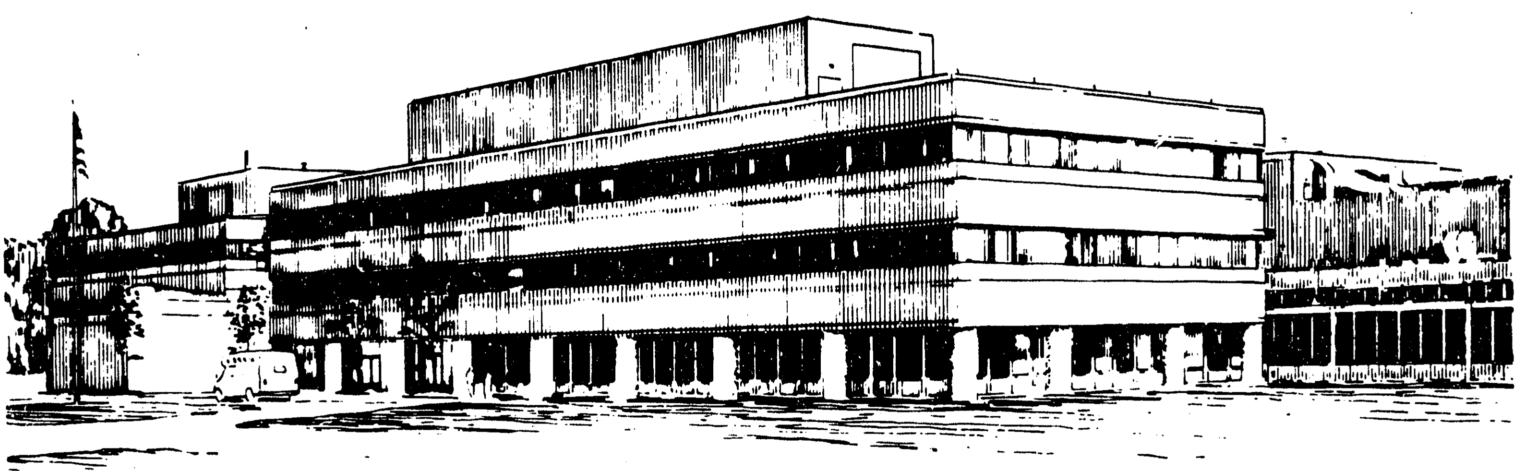

PRINCETON UNIVERSITY, PRINCETON, NEW JERSEY

ION CYCLOTRON RANGE OF FREQUENCY HEATING ON THE TOKAMAK FUSION TEST REACTOR

G. Taylor, M.G. Bell, H. Biglari, M. Bitter, N.L. Bretz, R. Budny, L. Chen, D. Darrow, P.C. Efthimion, D. Ernst, E. Fredrickson, G.Y. Fu, B. Grek, L. Grisham, G. Hammett, J.C. Hosea, A. Janos, D. Jassby, F.C. Jobes, D.W. Johnson, L.C. Johnson, R. Majeski, D.K. Mansfield, E. Mazzucato, S.S. Medley, D. Mueller, R. Nazikian, D.K. Owens, S. Paul, H. Park, C.K. Phillips, J.H. Rogers, G. Schilling, J. Schivell, G. L. Schmidt, J.E. Stevens, B.C. Stratton, J.D. Strachan, E. Synakowski, J.R. Wilson, K.L. Wong, and S.J. Zweben

Princeton Plasma Physics Laboratory, Princeton, New Jersey 08543

L. Baylor, C.E. Bush, R.C. Goldfinger, D.J. Hoffman, M. Murakami, A.L. Qualls, D. Rasmussen

Oak Ridge National Laboratory, Oak Ridge, Tennessee 08731

J. Machuzak

Massachusetts Institute of Technology, Cambridge, Massachusetts 02139

F. Rimini

JET Joint Undertaking, Abingdon, Oxfordshire, UK

Z. Chang

University of Wisconsin, Madison, Wisconsin 53706

Abstract

The complete ion cyclotron range of frequency (ICRF) heating system for the Tokamak Fusion Test Reactor (TFTR) [Fusion Tech. **21**, 1324 (1992)], consisting of four antennas and six generators designed to deliver 12.5 MW to the TFTR plasma, has now been installed. Recently a series of experiments has been conducted to explore the effect of ICRF heating on the performance of low recycling, Supershot plasmas in minority and non-resonant electron heating regimes. The addition of up to 7.4 MW of ICRF power to full size (R ~ 2.6 m, a ~ 0.95 m), helium-3 minority, deuterium Supershots heated with up to 30 MW of deuterium neutral beam injection has resulted in a significant increase in core electron temperature (ΔT_e=3-4 keV). Simulations of equivalent deuterium-tritium (D-T) Supershots predict that such ICRF heating should result in an increase in $\beta_\alpha(0)$ ~ 30%. Direct electron heating has been observed and has been found to be in agreement with theory. ICRF heating has also been coupled to neutral beam heated plasmas fueled by frozen deuterium pellets. In addition ICRF heated energetic ion tails have been used to simulate fusion alpha particles in high recycling plasmas. Up to 11.4 MW of ICRF heating has been coupled into a hydrogen minority, high recycling helium plasma and the first observation of the toroidal Alfvén eigenmode (TAE) instability driven by the energetic proton tail has been made in this regime.

PACS# 52.55.Fa 52.50.Gj

I. INTRODUCTION

A primary goal of the ion cyclotron range of frequency (ICRF) program on the Tokamak Fusion Test Reactor (TFTR)[1] is to enhance the alpha particle parameters in future deuterium-tritium (D-T) plasma experiments. Significant increases in the central α pressure ($\beta_\alpha(0)$) can be expected to result from the strong core electron heating induced by ICRF in a D-T neutral-beam heated plasma. Further, the suppression of the sawtooth instability and other magneto hydrodynamic (MHD) modes by localized ICRF heating may also increase plasma performance at the highest plasma currents and pressures in D-T experiments. In addition the generation of energetic minority tails by ICRF allows the simulation of D-T plasma alpha particle physics in a deuterium plasma. Beyond these immediate D-T physics goals, the TFTR ICRF program seeks to explore regimes which may impact the design of future devices, such as direct electron heating which does not require a diluting minority ion species.

This paper is an overview of results from several recent experiments which study different plasma regimes, including high-recycling, gas-fueled discharges, neutral beam injection (NBI) fueled Supershot plasmas, and pellet fueled discharges. Section II summarizes the technical aspects of the ICRF system on TFTR, including a description of recent improvements to the hardware and an assessment of the system performance. Section III presents results and observations from the ICRF plasma heating experiments on TFTR. Section IV provides a brief summary of this work.

II. TECHNICAL ASPECTS AND PERFORMANCE OF ICRF ON TFTR

The present ICRF antenna configuration consists of four antennas mounted on adjacent outboard midplane ports. Each antenna has two toroidally separated, radiating poloidal current elements. Six radio frequency (RF) generators feed the antennas, two of the antennas have one generator per element while the other two antennas have a single generator feeding both elements, with power division and phasing occurring in external sections of resonant transmission line which fix the antennas in an out-of-phase configuration. To date a fixed frequency of 47 MHz has been used at power levels up to 11.4 MW in high-recycling, L-mode plasmas. This operating frequency allows helium-3 fundamental minority or second harmonic tritium heating at the full TFTR toroidal magnet current (4.8T at R=2.62 m) which produces a resonant field for helium-3 at a major radius of 2.75m. The fundamental hydrogen minority resonance is also available at the same major radius for a reduced magnetic field (3.2 T at R=2.62 m).

Earlier ICRF experiments[2] with only two antennas, each with a significantly different design, revealed a notable difference in antenna loading impedance with one antenna delivering considerably less power than the other. Possible explanations for this difference may include differences in the k_z spectra, radial build of the antenna and the toroidal location relative to the plasma limiters. The poorer performing antenna was rebuilt to resemble the other as closely as possible and as a result both antennas were found to perform well, with total delivered powers up to 7 MW. The two new antennas installed in 1992 were based on this successful design, although the radial build and Faraday shield design were modified to reduce the separation between the plasma and the radiating elements. The k_z spectrum was improved by doubling the slots in the side walls and the mechanical support for the Faraday screen was reduced to a structure consisting of a series of radial rods. Although these design changes improved the k_z spectral purity, the mutual coupling between the radiating elements was increased by a factor of three, essentially limiting the new antenna configuration to either in-phase or out-of-phase operation. The other major design change was to slant the Faraday screen elements on the two new antennas at an angle of six degrees to better align the antennas with the total magnetic field used for normal plasma operation. To date the two new antennas have each operated well at power levels of 2.8 MW.

III. RESULTS AND OBSERVATIONS FROM ICRF EXPERIMENTS

A. L-Mode Discharges

Experiments which employ hydrogen minority ICRF heating of helium plasmas have recently been extended to RF power levels above 11 MW. Earlier work[3] with RF powers up to 6 MW in this regime had established a global confinement time for these plasmas which was enhanced over L-mode[4] by 20-30% due to the presence of the well confined 500-800 keV nonthermal hydrogen tail. However at higher power levels we observe a distinct saturation of global stored energy (Fig. 1), with global energy confinement dropping to close to the L-mode level at the highest RF powers. One explanation for this behavior is that as the RF power is increased, the minority ions become more energetic and therefore develop larger banana widths. The minority ions then spend more time further from the plasma core where their slowing down time is shorter and hence the tail stored energy saturates resulting in a saturation in the global stored energy[5]. The observed saturation may also result from an enhanced fast ion loss due to interaction of the minority ions with the toroidal Alfvén eigenmode (TAE); which is discussed further in section IIIE.

B. Minority ICRF Heating of Supershot Plasmas

A major physics objective of the ICRF heating experiments on TFTR is to enhance the performance of plasmas during the D-T plasma phase which is scheduled to commence in 1993. Since 1986, Supershot plasmas have provided the highest reactivity regime on TFTR[6]. However, the Supershot plasma regime was originally established in NBI plasmas at a major radius of 2.45 m and a minor radius of 0.8 m. In order to couple ICRF power into these plasmas it has been necessary to develop a larger Supershot plasma with a major radius ~ 2.6 m and minor radius ~ 0.95 m so that the outer plasma edge is within 1-2 cm of the ICRF antennas while the power flow from the plasma continues to be deposited on the inboard limiter. In past runs, operating at the larger radius generally degraded the reactivity compared to 2.45 m plasmas at the same NBI power level. Further, in order to minimize the power flow to the outboard limiter, which has poorer power handling capability than the inboard limiter, an additional variable curvature (VC) field had been used to increase the plasma oblateness. This increased oblateness moves the outboard, midplane, plasma edge towards the ICRF antennas, while the top and bottom of the plasma move away from the outboard limiter. But application of the VC field also significantly degrades plasma performance, either because of increased gas influx or reduced MHD stability. Recently, as a result of extensive plasma conditioning, good plasma reactivity was achieved in these larger Supershots, with global confinement times 2.5-3 times the L-mode value[1]. As a result of this improved confinement it was possible to obtain the plasma oblateness necessary for good ICRF coupling through improved plasma β, rather than with the application of an external VC field.

Because Supershot plasmas are low recycling discharges they have low edge densities which make them technically challenging from the standpoint of ICRF heating. Optimal ICRF coupling requires densities in front of the antenna which are approximately $5 \times 10^{17} m^{-3}$. Due to the rapid density rise which accompanies the first ~ 0.3 sec of NBI, the loading impedance on the ICRF antennas increases by a factor of 5-6. Also eigenmodes of the plasma filled vacuum vessel cavity are observed during helium-3 minority heating when ICRF is applied early in the NBI pulse, this causes spikes in the reflected power which can shutdown the RF sources. These phenomena make it inherently difficult to couple ICRF into Supershots early in the NBI pulse. The antenna coupling was optimized by exploring the effect of plasma radial position and shaping. The front end of the ICRF pulse was modified to provide a relatively modest ramp of RF power early in the NBI pulse which minimized problems associated with eigenmodes and the rapid change in RF loading impedance at the start of NBI.

ICRF heating applied during the NBI pulse can improve the performance of TFTR D-T Supershot plasmas in two ways. The increased core electron temperature produced by ICRF will increase the alpha particle slowing down time and hence $\beta_\alpha(0)$ for the same alpha particle source rate. In addition the ICRF can suppress sawteeth which limit performance at the high plasma currents ($I_p \sim 2.5$ MA) required to avoid β limits at the highest available NBI powers. When ICRF is applied in the hydrogen minority regime to a deuterium plasma, increased reactivity also occurs as a result of second harmonic heating of deuterium beam ions. However this effect will be less pronounced in a D-T plasma where NBI energies (~100keV) are near the peak of the D-T fusion cross-section.

Most of the recent work on the ICRF heating of deuterium Supershots in TFTR has taken place in the helium-3 minority regime which can be used at the full toroidal magnetic field with the present 47 MHz heating system. Figure 2 shows a comparison between two deuterium Supershots with a helium-3 minority, both with 23 MW of NBI between 3 and 4 seconds. Sawtooth activity was suppressed even in the plasma with only NBI power applied. One of these discharges (dashed line) had 5.7 MW of ICRF heating coupled into it between 3.2 and 4 seconds. The central electron temperature increases by 40% and the global stored energy increases by 20% with the addition of ICRF. With the application of ICRF the core ion temperature at 3.7 seconds increased from 19 to 21 keV, however this difference is within the uncertainties of the measurement. The neutron production rate is very similar for both plasmas and is predominantly the result of beam-beam and beam-target ion reactions, less than 10% results from thermal ion reactions. The insensitivity of the neutron production rate to an increase in core electron temperature is expected; since the core electron temperature is high (>9keV), even without ICRF heating, the critical energy for the deuterium beam ions is already ~200 keV. The calculated slowing down time for the neutral beam full-energy component is ~150 msec at 3.7 sec for both plasmas. The confinement time and central electron density evolution are similar in both discharges, however there is a small (~10%) increase in Z_{eff} with the application of ICRF heating. An increase in titanium concentration is measured during the ICRF pulse which is consistent with some impurities coming from the antennas. But the titanium increase is insufficient to account for the rise in Z_{eff}. The increased Z_{eff} probably results from a combination of impurity influx from the limiter and the antennas. It is important to minimize this impurity influx during the ICRF pulse since it will lead to reduced reactivity. The relatively small increase in impurities measured here results from the beneficial effect of extensive antenna conditioning which preceded these experiments. Figure 3 shows the response of the electron temperature profile to the application of ICRF power and the calculated electron power deposition profile plotted against normalized minor radius (r/a) at the time indicated in Fig.2. ICRF power increases the electron temperature in a region which extends out to $r/a \approx 0.4$. The electron power deposition (Q_e) was calculated with a time dependent transport code (TRANSP[7]) and was found to increase significantly in the core region from $0.4 MW/m^3$ with NBI only, to $1.4 MW/m^3$ with the addition of ICRF. A D-T plasma simulation has been performed for this pair of discharges. In these simulations deuterium beams which were oriented counter to the plasma current (~40% of the applied NBI power) were replaced by tritium beams. Figure 4 shows that the central alpha particle slowing down time increases by over 50% with the application of ICRF. The average increase for the volume inside $r/a \approx 0.15$ is about 30%. A D-T TRANSP projection out to 4.3 seconds which assumes constant plasma parameters (i.e. with the NBI and RF heating pulses extended by 0.3 seconds) gave an equilibrium $\beta_\alpha(0)$ increase of 30% with the addition of ICRF heating. Experiments conducted at higher plasma currents (I_p=2.2MA) and higher NBI powers (~ 30MW) have demonstrated ICRF suppression of sawtooth activity, in addition to significant core electron heating (~3-4 keV), with up to 7.4 MW of ICRF power.

C. Pellet Fueled Neutral Beam Heated Plasmas

For the TFTR D-T physics phase, a tritium pellet injector will provide an alternate and more efficient source of tritium fueling than can be accomplished with the tritium NBI alone. In these pellet fueled D-T discharges, a tritium pellet will fuel the plasma before deuterium NBI. A complication of this scenario is that as the deuterium NBI pulse evolves, the tritium concentration will be decreasing. The pellet initially cools the plasma, and in order to maximize plasma reactivity early in the NBI pulse, the electron temperature at the start of NBI needs to be enhanced. ICRF heating can enhance the plasma reheat following pellet injection and provide a high temperature target plasma for the NBI. In recent experiments, a comparison was made between a plasma with pellet injection followed by NBI and one where ICRF was added to assist the reheat following pellet injection. Fig. 5 shows some results from these initial experiments. An ICRF power of 4.5 MW was coupled into the plasma from 200 msec after pellet injection to the end of NBI. Just before pellet injection the density profile of the plasma without ICRF was slightly more peaked than the one with ICRF and this remained the case following pellet injection up to the start of NBI. During NBI however the density profile was almost identical in both plasmas. The core electron temperature attained in the plasma with ICRF heating was enhanced by 4-5 keV both before and during NBI. Since the electron temperature in the core of the plasma without ICRF was only ~3.5 keV just before NBI the elevated core electron temperature, obtained with ICRF heating, increased the slowing down time of the ~100 keV beam ions, and as a result the neutron production rate was enhanced by 25%.

D. Direct Electron Heating

Direct electron heating has significant potential for D-T experiments since no minority species is added to dilute the reactive ions. Further, energetic tail ions generated during helium-3 minority ICRF heating can complicate alpha particle measurements; direct electron heating avoids this difficulty. Also, for future machines direct electron damping offers the possibility of a practical current drive mechanism for steady state fusion devices. On TFTR, two regimes of direct electron heating have been explored. The results obtained are similar to earlier work.[8,9] Since the direct electron heating mechanism is relatively weak, it is essential to minimize competition from ion cyclotron resonances in the plasma. Competing ion resonances in the low field regime (2.3T) are the fundamental hydrogen resonance located on the high field plasma boundary, the second harmonic helium-3 resonance in the core, and the third harmonic deuterium resonance towards the low field side. In the high field regime (4.7T) there is competition from the fundamental helium-3 resonance in the core, and the deuterium fundamental and shear Alfvén resonances near the high field plasma boundary.

In the low field experiments, a helium-3 plasma was employed, and the RF power was 100% modulated with a 4 Hz square wave. The time history of the central electron temperature determined from electron cyclotron emission measurements showed significant core heating. From the rate of change of the electron temperature ($\Delta(dT_e/dt)$) when the RF power changed it is possible to calculate the local power deposition on the electrons, Q_e. It was assumed that the electron heat transport remained constant in time and there was no sudden discontinuity in the electron density. The deposition was then calculated using the equation $Q_e = 1.5n_e\Delta(dT_e/dt)$. A second, Fourier transform technique was also used to determine Q_e. It gave good agreement with the rate of change method, indicating that the rise and fall times of the RF modulation was faster than the characteristic energy transport time. Approximately 30-50% of the RF power was determined to have directly heated electrons in this regime. The deposition profile shape is consistent with that predicted by a combination of transit-time magnetic pumping and electron Landau damping. The remainder of the RF power is assumed to be absorbed by ion resonances, in particular the hydrogen fundamental resonance. Ion temperature evolution measurements which employ charge exchange recombination from carbon ions show only a weak response to the RF modulation consistent with minimal second harmonic helium-3 absorption. Vertically viewing neutron collimator measurements indicate some third harmonic deuterium absorption on the doping beam for the ion temperature measurement.

High field experiments used a deuterium plasma in which the only ion resonance was a weak deuterium resonance on the high field side. Figure 6 shows the RF power waveform, and the time evolution of the electron temperature at the magnetic axis and half way towards the edge. A 5 Hz square wave modulated the 1.5 MW RF pulse. Theory predicts that β_e needs to be maximized in order to get reasonable single pass absorption; this was accomplished by preheating the discharge with 24 MW of NBI. There is a clear modulation of the central electron temperature (ΔT_e~1.5 keV) by the RF power. Once again the electron temperature data were analyzed by the two methods described earlier. As shown in Fig. 7, the rate of change analysis gave a centrally absorbed RF power which was 60% of the applied power. The Fourier transform method gave a similar result, but could only be used to determine core deposition due to low signal in the outer half of the discharge. The integrated power deposition to the electrons (P_e) determined by the rate of change of electron temperature was found to be similar to the applied RF power. Modeling with a three dimensional, full wave spectral code (PICES[10]) indicates that ~ 80% of the power goes directly to the electrons, the rest is probably absorbed by the fundamental deuterium ion resonance.

E. Observation of MHD Modes Driven by RF Tail Ions

ICRF minority tails have the potential to simulate D-T alpha particle effects in D-D plasmas. ICRF driven minority tail energies extend to ~1 MeV and are therefore particularly well suited for the simulation of alpha-particle driven instabilities such as the toroidal Alfvén eigenmode (TAE) instability. Earlier work has already shown that the TAE mode can be driven at low toroidal magnetic fields by ~ 100 keV passing NBI ions[11,12], but this mode is also expected to be driven by trapped ions[13]. Experiments have been performed on TFTR in helium L-mode plasmas to investigate the trapped-particle-driven TAE mode. ICRF heating was used to create an energetic (500-700 keV) minority tail at $B_T(0) = 3.2$ T, $I_p = 1.3$-1.85 MA and average electron densities were in the range 1.5-4x10^{19} m^{-3}. The behavior of the trapped particle driven TAE mode appears similar to the behavior observed previously for the NBI driven TAE mode in TFTR[11]. The RF power threshold for driving the instability under these conditions was found to be about 3 MW. At this power level, the stored energy in the minority tail was about 100 kJ, corresponding to a threshold $\langle\beta_{tail}\rangle_{vol} \sim 0.03\%$, comparable to the theoretically derived threshold. With ~3MW of RF power the instability is observed 100 msec after RF is coupled into the plasma; at higher RF powers the delay shortens, consistent with a critical β_{tail} for driving the instability. The instability was measured by both the Mirnov coil system and the microwave reflectometer[14] as shown in Fig. 8. The observed instability frequencies lie in the range 150-200 kHz, have a narrow spectral spread and scale with the TAE mode frequency, $\omega = v_A/2qR$ when v_A is calculated with the density at the $q = 1.5$ surface. Both the reflectometer and Mirnov coil data show multiple instability frequencies presumably due to multiple toroidal modes.

Figure 9 shows a distinct threshold for the instability as the RF power is increased from 2 to 3 MW. This figure also shows that the instability can be modulated by other MHD modes, such as sawteeth. This modulation may be the consequence of local variations in the energetic ion pressure gradient. The lost-ion probe signal amplitude correlates with the envelope of the oscillations measured with the Mirnov coil system. A relatively small fast ion loss (~1%) is seen by lost ion probes at each sawtooth crash. However, as the RF power is increased from 3 to 11 MW the fast ion loss fraction increases by an order of magnitude. The fast ion losses at the highest RF power levels studied so far may be a significant fraction of the fast ion population; which may explain the observed saturation of stored energy for RF powers above ~7MW shown in Fig. 1. Collisional damping due to interaction between electrons at the trapped/passing boundary is believed to be the dominant wave damping mechanism. If so, then ~ 500 kJ of tail energy would be required to destabilize the instability at the full TFTR magnetic field. It should be possible to achieve this tail energy level with the present ICRF system in the helium-3 regime without NBI. In D-T NBI plasmas ion Landau damping may quench the instability due to the increased ion pressure.

IV. SUMMARY

The operational capability of the ICRF heating system on TFTR has recently been enhanced with the addition of two new antennas, and a new maximum RF power level of 11.4 MW has been coupled into TFTR discharges. ICRF heating of DD Supershot plasmas with RF powers up to 7.4 MW has resulted in a significant enhancement of the core electron temperature, ΔT_e=3-4 keV, and ICRF suppression of sawtooth activity. Modeling of these plasmas indicates that this enhancement extrapolates to an increase in $\beta_\alpha(0)$ ~ 30% for a D-T plasma. An experimental scenario which combines ICRF heating with pellet fueling and NBI is being developed for the D-T phase of TFTR where tritium pellet injection will be used to provide efficient core fueling. Direct electron heating has been measured in both low and high toroidal field regimes where ion resonances exist only at the plasma edge. Up to 80% absorption of the

RF power by direct electron damping has also been observed in this regime. An ICRF minority tail has excited the trapped-particle-driven TAE mode in an L-mode plasma and a significant enhancement in the fast ion loss fraction has been measured with increasing RF power when the mode is p.

ACKNOWLEDGEMENTS

The authors would like to thank the ICRF group and TFTR project engineering and technical staff for their contribution to this work. We are grateful to Drs. R. Davidson, R. Hawryluk, H. Furth, D. Meade, and P. Rutherford for their continued support of the ICRF research program. This work was funded by U.S. Department of Energy contract No. DE-AC02-76-CHO-3073.

REFERENCES

1. R.J. Hawryluk, D. Mueller, J.C. Hosea, C.W. Barnes, M. Beer, M.G. Bell, R. Bell, H. Biglari, M. Bitter, R. Boivin, N.L. Bretz, R. Budny, C.E. Bush, L. Chen, C.Z. Cheng, S. Cowley, D.S. Darrow, P.C. Efthimion, R.J. Fonck, E. Fredrickson, H.P. Furth, G. Greene, B. Grek, L.R. Grisham, G. Hammett, W.W. Heidbrink, K.W. Hill, D. Hoffman, R.A. Hulse, H. Hsuan, A. Janos, D.L. Jassby, F. Jobes, D.W. Johnson, L.C. Johnson, R. Kaita, J. Kamperschroer, J. Kesner, C.K. Phillips, S.J. Kilpatrick, H. Kugel, B. LeBlanc, P.H. La Marche, D.M. Manos, D.K. Mansfield, E.S. Marmar, E. Mazzucato, M.P. McCarthy, J. Machuzak, M. Mauel, D.C. McCune, K. McGuire, S.S. Medley, D.R. Mikkelsen, D. Monticello, Y. Nagayama, G.A. Navratil, R. Nazikian, D.K. Owens, H. Park, W. Park, S. Paul, F. Perkins, S. Pitcher, D. Rasmussen, M.H. Redi, G. Rewoldt, D. Roberts, A.L. Roquemore, S. Sabbagh, G. Schilling, J. Schivell, G.L. Schmidt, S.D. Scott, J. Snipes, J. Stevens, B.C. Stratton, J.D. Strachan, W. Stodiek, E. Synakowski, W. Tang, G. Taylor, J. Terry, J.R. Timberlake, H.H. Towner, M. Ulrickson, S. von Goeler, R. Wieland, J.R. Wilson, K-L. Wong, P. Woskov, M. Yamada, K.M. Young, M.C. Zarnstorff, and S.J. Zweben, Fusion Tech. **21**, 1324 (1992).

2. J.C. Hosea, P. Bonanos, P. Colestock, G. Greene, S.S. Medley, C.K. Phillips, J. Stevens, J.R. Wilson, W. Gardner, D. Hoffman, and D. Swain, in *Proceedings 8th Topical Conference on Radio Frequency Power in Plasmas,* Irvine (American Institute of Physics, New York, 1989), p.278.

3. J.R. Wilson, J.C. Hosea, M.G. Bell, M. Bitter, R. Bovin, E.D. Fredrickson, G.J. Greene, G.W. Hammett, K.W. Hill, D.J. Hoffman, H. Hsuan, M. Hughes, A.C. Janos, D.L. Jassby, F.C. Jobes, D.W. Johnson, C.K. Phillips, D.K. Mansfield, K. M. McGuire, S.S. Medley, D. Mueller, Y. Nagayama, M. Ono, D.K. Owens, H.K. Park, M. Phillips, A.T. Ramsey, G. L. Schmidt, S.D. Scott, J.E. Stevens, B.C. Stratton, E. Synakowski, G. Taylor, M. Ulrickson, K.L. Wong, M.C. Zarnstorff, and S.J. Zweben, Phys. Fluids B **3**, 2270 (1991).

4. R.J. Goldston, Plasma Phys. **26**, 87 (1984).

5. G.A. Cottrell and D.F.H. Start, Nucl. Fusion **31**, 61 (1991).

6. J.D. Strachan, M. Bitter, A.T. Ramsey, M.C. Zarnstorff, V. Arunasalam, M.G. Bell, N.L. Bretz, R. Budny, C.E. Bush, S.L. Davis, H.F. Dylla, P.C. Efthimion, R.J. Fonck, E. Fredrickson, H.P. Furth, R.J. Goldston, L.R. Grisham, B. Grek, R.J. Hawryluk, W.W. Heidbrink, H.W. Hendel, K.W. Hill, H. Hsuan, K.P. Jaehnig, D.L. Jassby, F. Jobes, D.W. Johnson, L.C. Johnson, R. Kaita, J. Kamperschroer, R.J. Knize, T. Kozub, H. Kugel, B. LeBlanc, F. Levinton, P.H. La Marche, D.M. Manos, D.K. Mansfield, K. McGuire, D.H. McNeill, D.M. Meade, S.S. Medley, W. Morris, D. Mueller, E.B. Nieschmidt, D.K. Owens, H. Park, J. Schivell, G. Schilling, G.L. Schmidt, S.D. Scott, S. Sesnic, J.C. Sinnis, F.J. Stauffer, B.C. Stratton, G.D. Tait, G. Taylor, H.H. Towner, M. Ulrickson, S. von Goeler, R. Wieland, M.D. Williams, K-L. Wong, S. Yoshikawa, K.M. Young, and S.J. Zweben, Phys. Rev. Lett. **58**, 1004 (1987).

7. D.N. Smithe, C.K. Phillips, G.W. Hammett, and P.L. Colestock, in *Proceedings 8th Topical Conference on Radio Frequency Power in Plasmas,* Irvine (American Insitute of Physics, New York, 1989), p. 338. G.W. Hammett, Ph.D. Thesis, Princeton University (1986), available from University Microfilms, Ann Arbor MI 48105 (USA).

8. J. Jacquinot and the JET Team, Plasma Physics **33**, 1657 (1991).

9. C.C. Petty, R.I. Pinsker, M.J. Mayberry, S.C. Chiu, T.C. Luce, R. Prater, J.C.M. de Haas, R.A. James, F.W. Baity, R.H. Goulding, D.J. Hoffman, P.T. Bonoli, and M. Porkolab, in *Proceedings 9th Topical Conference on Radio Frequency Power in Plasmas,* Charleston (American Institute of Physics, New York,1992), p.96.

10. E.F. Jaeger and D.B. Batchelor, in *Proceedings 9th Topical Conference on Radio Frequency Power in Plasmas,* Charleston (American Institute of Physics, New York,1992), p.159.

11. K-L. Wong, R.J. Fonck, S.F. Paul, D.R. Roberts, E.D. Fredrickson, R. Nazikian, H.K. Park, M. Bell, N.L. Bretz, R. Budny, S. Cohen, G.W. Hammett, F.C. Jobes, D.M. Meade, S.S. Medley, D. Mueller, Y. Nagayama, D.K. Owens, and E.J. Synakowski, Phys. Rev. Lett. **66**, 1874 (1991).

12. W.W. Heidbrink, E.J. Strait, E. Doyle, G. Sager, and R.T. Snider, Nucl. Fusion **31**, 1635 (1991).

13. H. Biglari, F. Zonca, and L. Chen, Phys. Fluids B **4**, 2385 (1992).

14. E. Mazzucato, R. Nazikian, E. Fredrickson, K. McGuire and the TFTR Group, Bull. Am. Phys. Soc. **37**, 1484 (1992).

FIGURE CAPTIONS

Figure 1

Dependence of stored energy and energy confinement time on total heating power for an ICRF power scan into a I_p = 1.85 MA, $B_T(0)$ = 3.2 T, R = 2.62 m, a = 0.96 m helium plasma with a hydrogen minority species which had a fundamental resonance at R = 2.75 m. The stored energy is observed to saturate for ICRF powers greater than 6-7 MW and the global energy confinement time drops to close to the Goldston L-mode value at the highest RF powers.

Figure 2

Comparison of various major plasma parameters for two I_p = 1.85 MA, $B_T(0)$ = 4.8 T, R = 2.62 m, a = 0.96 m helium-3 minority, deuterium Supershot plasmas, one with NBI alone (solid line) the other with the addition of 5.7 MW of ICRF (dashed line). The fundamental resonant field location for helium-3 was at R = 2.75 m. A 3-4 keV electron temperature rise is measured in the plasma core with no change in plasma reactivity .

Figure 3

Comparison of radial profiles of electron temperature and power deposition calculated by TRANSP for the two plasmas shown in Fig. 2. ICRF provides significant core electron power deposition in a Supershot plasma.

Figure 4

Evolution of measured central electron temperature and projections of alpha particle slowing down time for a D-T plasma with the same parameters as the discharges shown in Figs. 2 and 3. The predictive analysis employed the time dependent transport code, TRANSP.

Figure 5

Time evolution of neutron production rate, central electron temperature and density for two plasmas each fueled by a deuterium pellet at 2.4 sec and 20 MW of NBI between 3 and 3.6 sec. An ICRF heating pulse was added to one of these plasmas (solid line) after pellet injection. ICRF heating significantly enhanced the electron temperature following pellet injection; and during NBI. Reactivity was enhanced during NBI in the plasma with ICRF heating.

Figure 6

Time evolution of RF power, electron temperature, central electron density and stored energy for a plasma which exhibits direct electron damping of ICRF. Efficient direct electron heating is seen in the core of a B_T = 4.7 T (at R= 2.82 m) deuterium Supershot plasma when 5 Hz modulated 47 MHz RF power is applied in the absence of a minority species. Modulation of the central electron temperature is evidence for significant core heating.

Figure 7

Power deposition profile analysis and volume integrated power at the time indicated in Fig. 6. Approximately 80% of the RF power is absorbed directly by electrons and the deposition profile shape is consistent with a combination of electron Landau damping and transit time magnetic pumping.

Figure 8

Observation of a mode consistent with the trapped particle driven TAE mode as seen (a) on the time evolution of the Mirnov coil spectrum and (b) on the frequency spectrum of density fluctuations measured at 2.6 seconds (the time indicated by the thick line in (a)) within 10 cm of the plasma center with a microwave reflectometer.

Figure 9

The signal from a lost particle probe at 45^o below the outer midplane, the amplitude of oscillations seen with the Mirnov coil system between 150 and 200kHz, central electron temperature measured by electron cyclotron emission and the ICRF power evolution. The TAE mode appears as the RF power transitions from 2.2 to 3.2 MW. The corresponding $<\beta_{tail}>_{vol}$ ~ 0.03% at an RF power ~ 3 MW. Relatively small (~1%) tail ion losses correlate with Mirnov signal behavior at each sawtooth crash at this RF power level, however at RF powers ~ 11 MW the fast ion loss fraction is approximately an order of magnitude larger

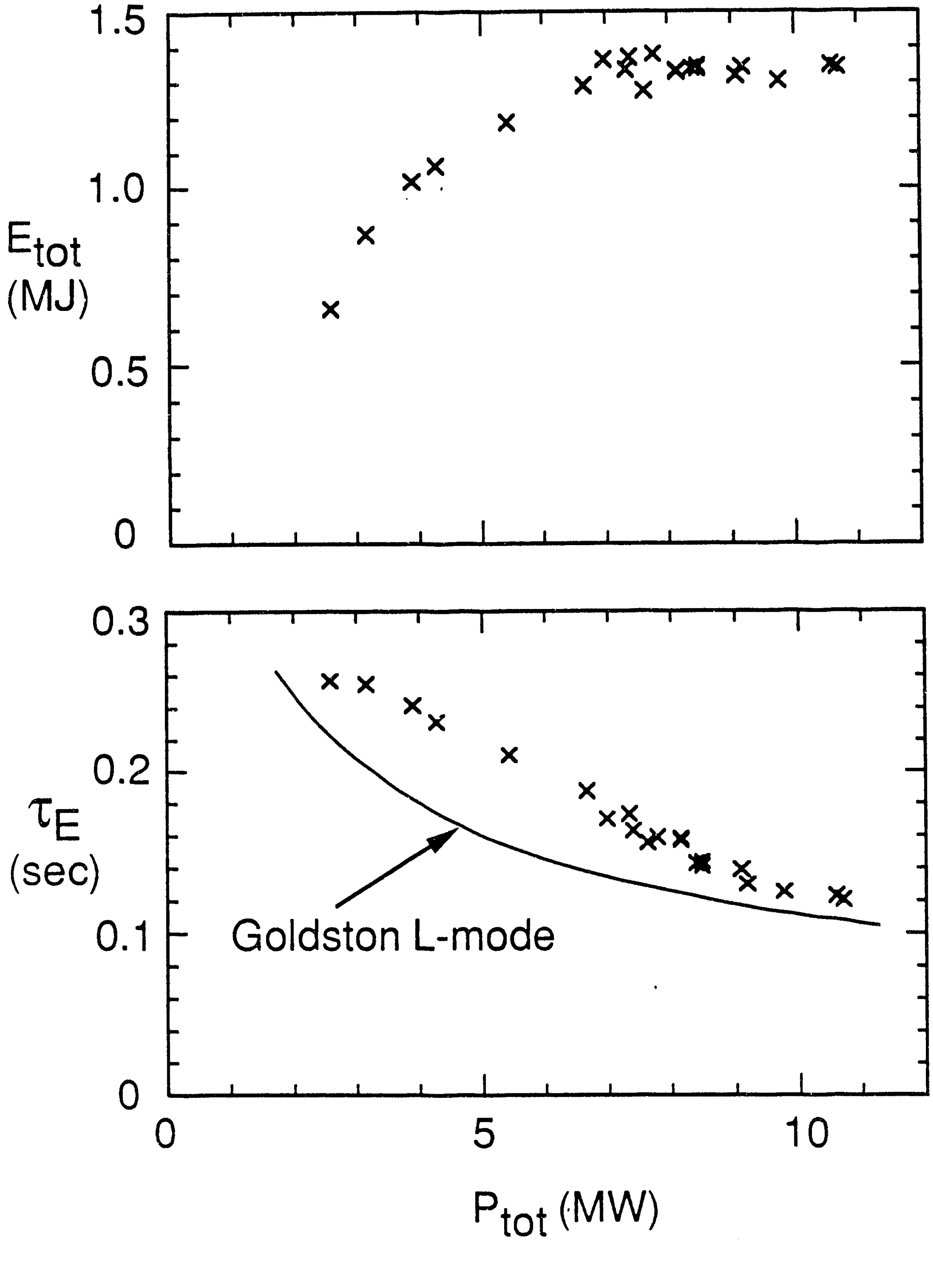
1.5
1.0
0.5
0
E_{tot}
(MJ)
0.3
0.2
0.1
0
τ_E
(sec)
Goldston L-mode
0
5
10
P_{tot} (MW)

Figure 1

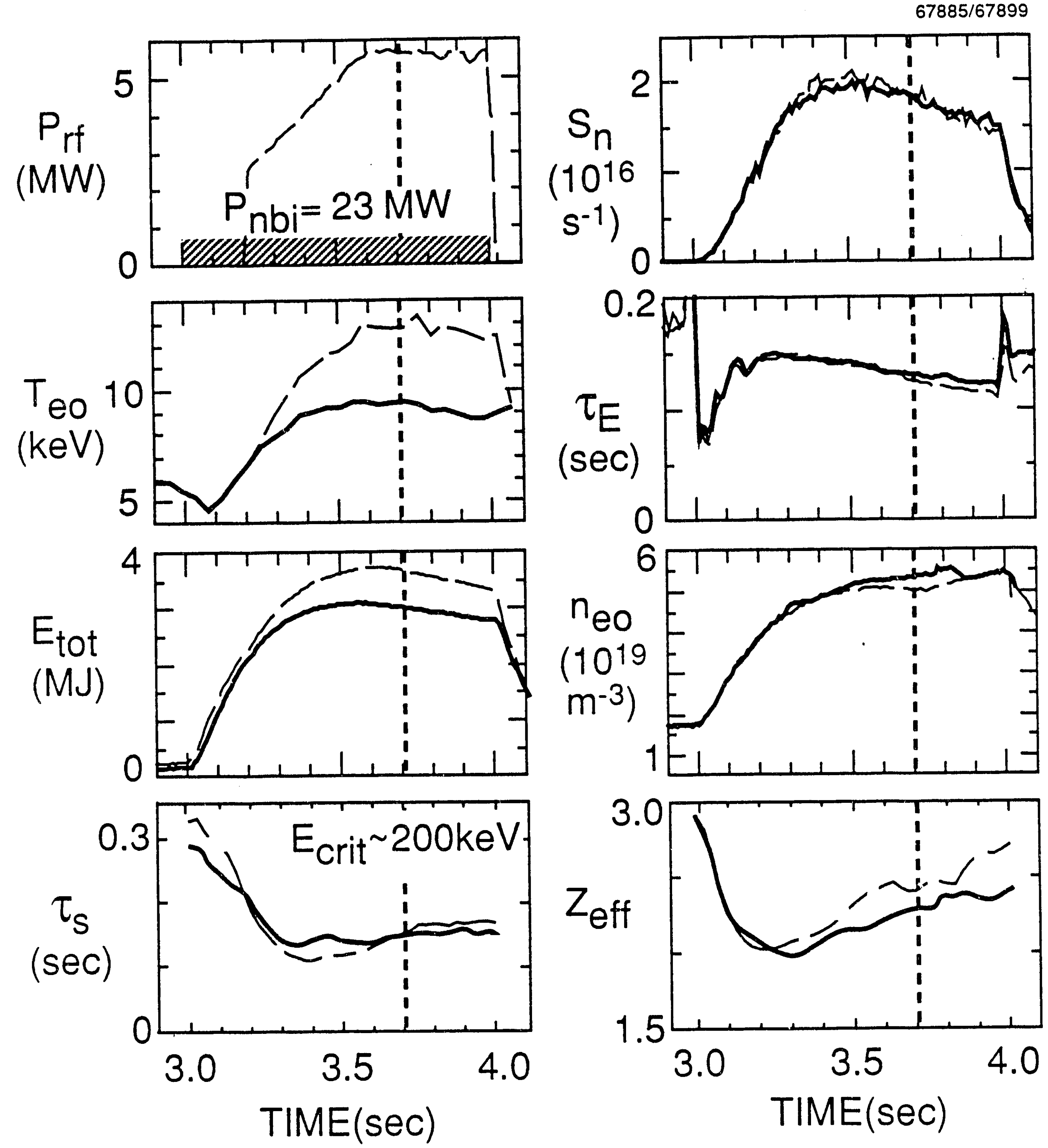
67885/67899
P_{rf} (MW)
P_{nbi}= 23 MW
T_{eo} (keV)
E_{tot} (MJ)
τ_s (sec)
E_{crit}~200keV
S_n (10^{16} s^{-1})
τ_E (sec)
n_{eo} (10^{19} m^{-3})
Z_{eff}
TIME(sec)
TIME(sec)

Figure 2

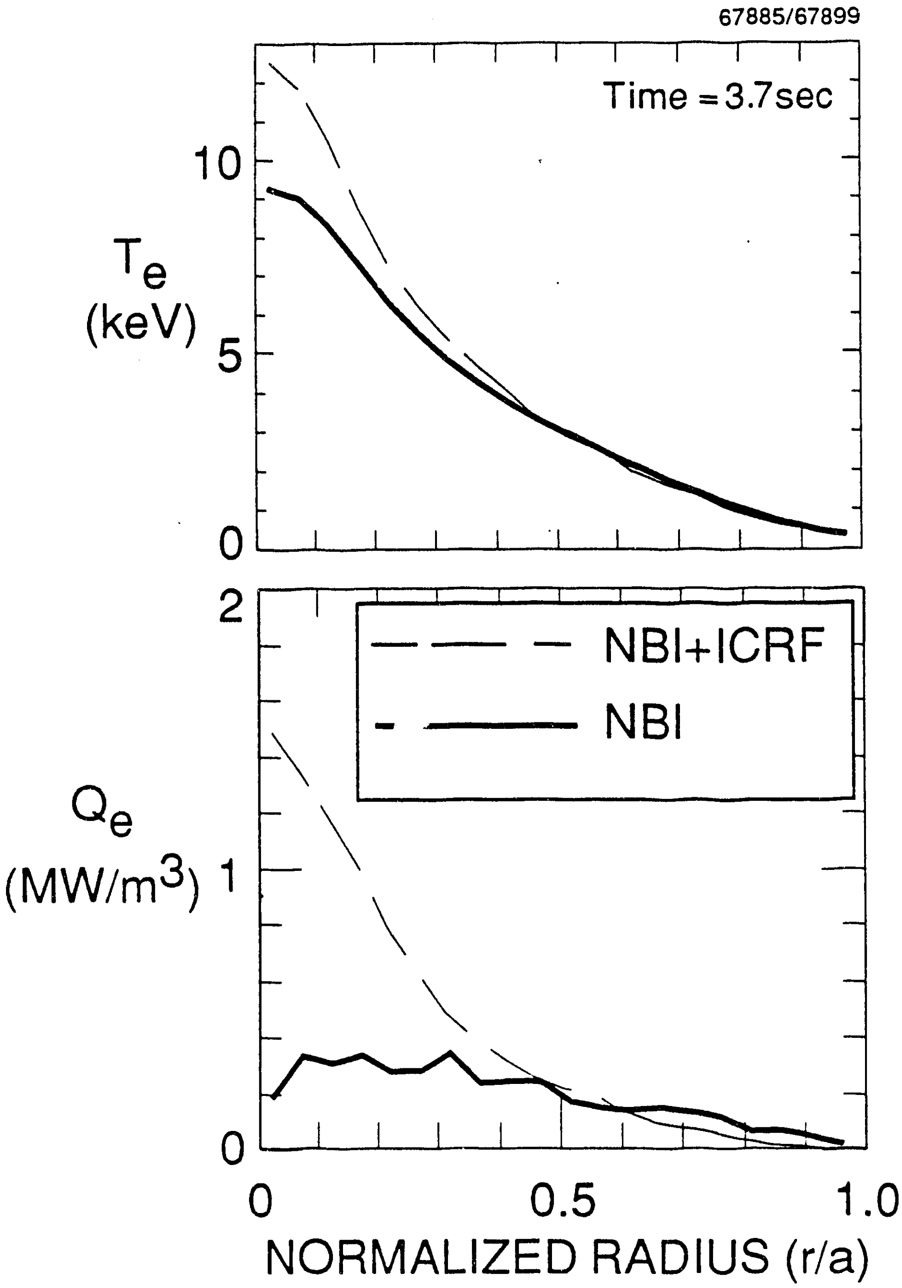

67885/67899
Time = 3.7sec
10
T_e
(keV)
5
0
2
NBI+ICRF
NBI
Q_e
(MW/m^3)
1
0
0
0.5
1.0
NORMALIZED RADIUS (r/a)

Figure 3

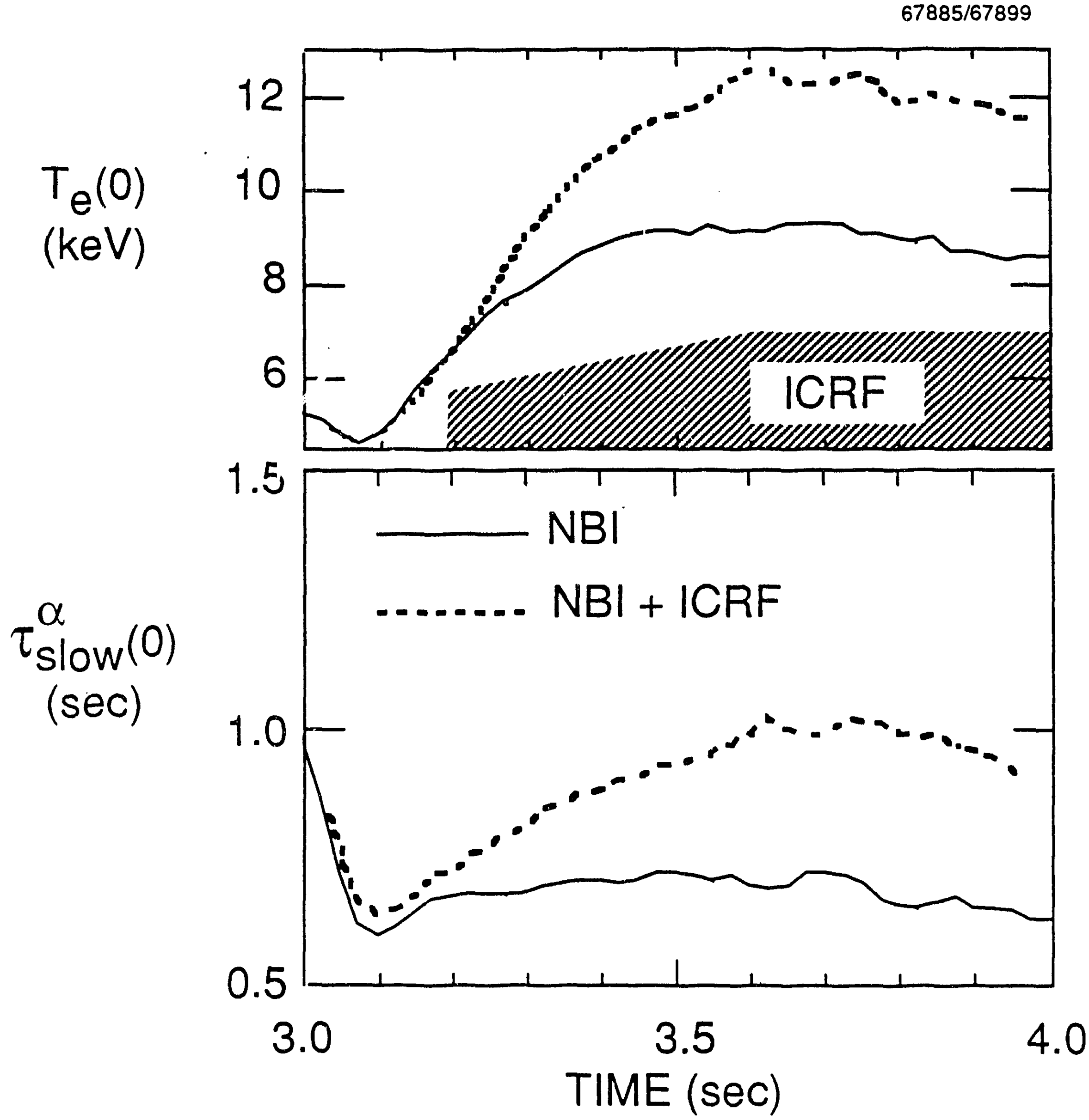
67885/67899
$T_e(0)$ (keV)
12
10
8
6
ICRF
1.5
NBI
NBI + ICRF
$\tau^{\alpha}_{slow}(0)$ (sec)
1.0
0.5
3.0
3.5
4.0
TIME (sec)

Figure 4

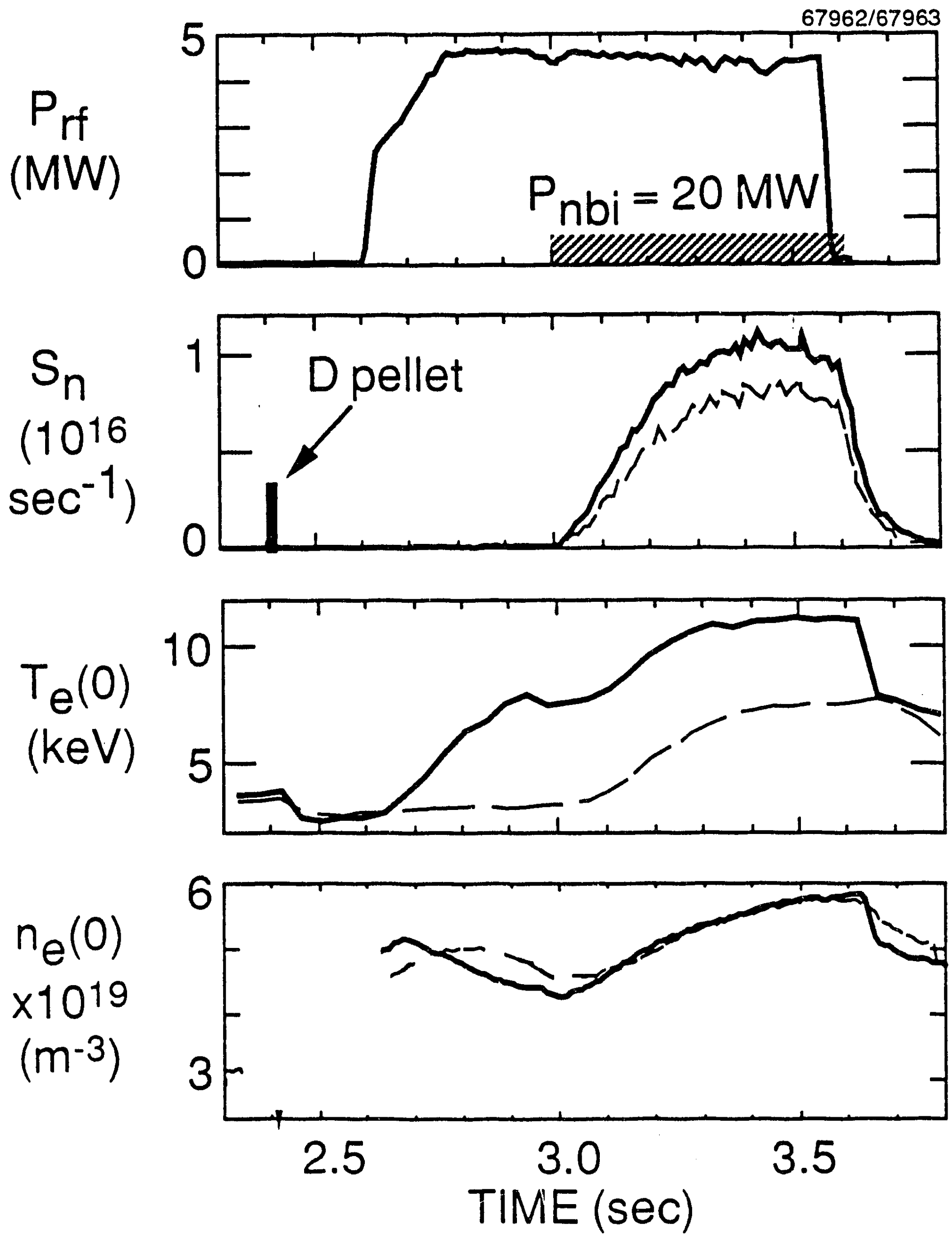

67962/67963
P_{rf} (MW)
5
0
P_{nbi} = 20 MW
S_n (10^{16} sec^{-1})
1
0
D pellet
$T_e(0)$ (keV)
10
5
$n_e(0)$ $x10^{19}$ (m^{-3})
6
3
2.5
3.0
3.5
TIME (sec)

Figure 5

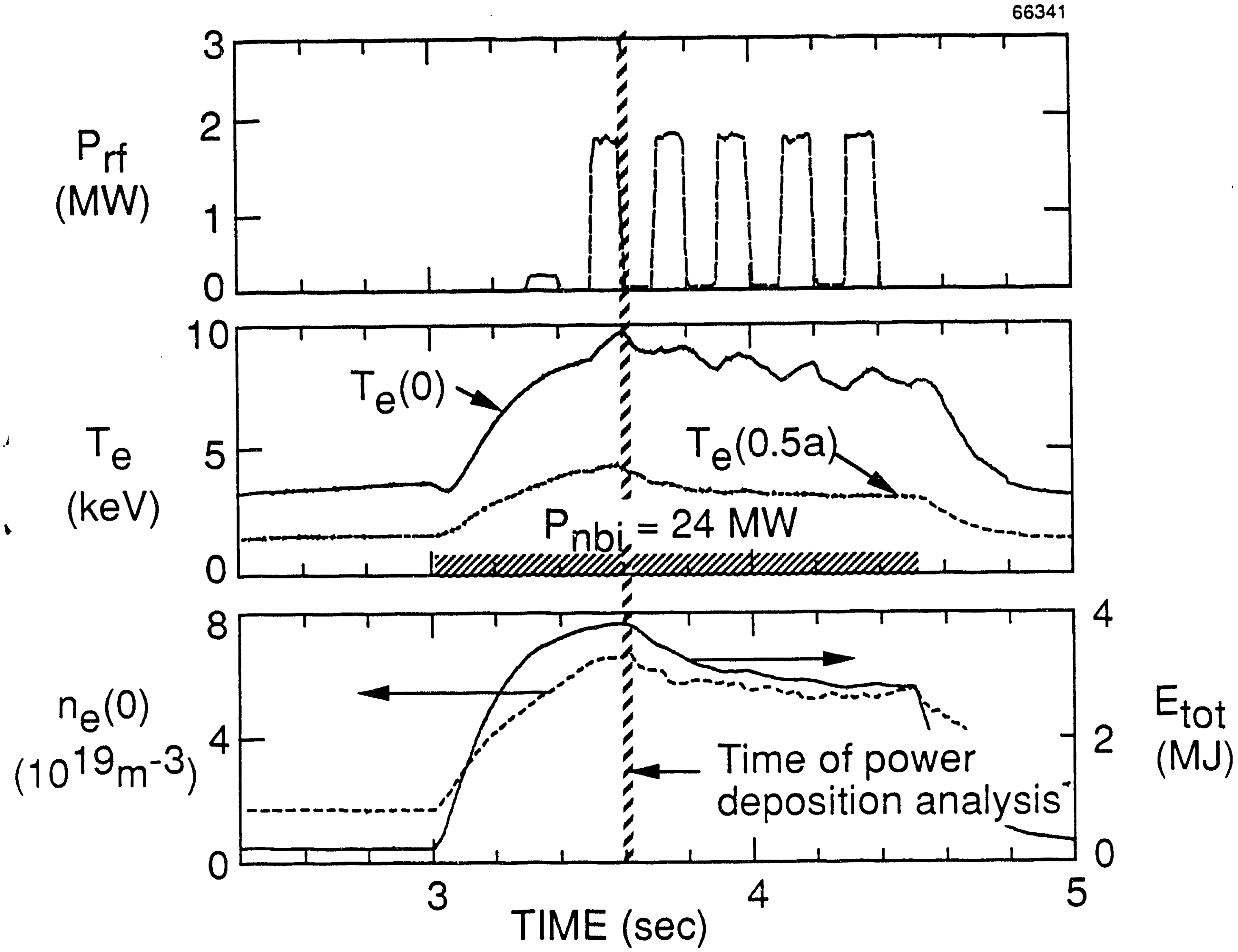
66341
P_{rf} (MW)
3
2
1
0
$T_e(0)$
T_e (keV)
10
5
0
$T_e(0.5a)$
P_{nbi} = 24 MW
$n_e(0)$ $(10^{19}m^{-3})$
8
4
0
E_{tot} (MJ)
4
2
0
Time of power deposition analysis
3
4
5
TIME (sec)

Figure 6

(a)

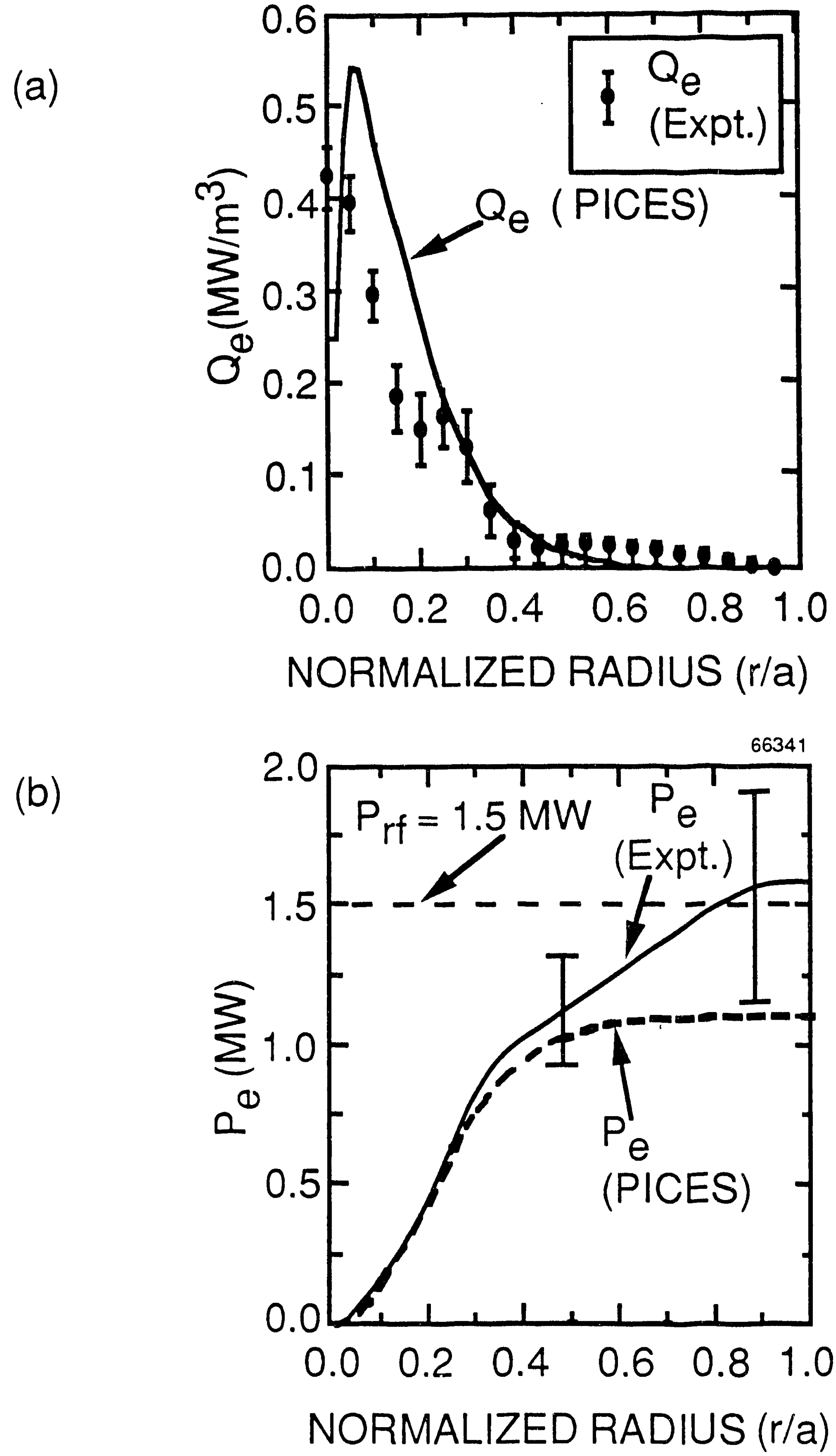

0.6
0.5
0.4
0.3
0.2
0.1
0.0
Q_e(MW/m^3)
Q_e
(Expt.)
Q_e (PICES)
0.0 0.2 0.4 0.6 0.8 1.0
NORMALIZED RADIUS (r/a)
(b)
66341
2.0
1.5
1.0
0.5
0.0
P_e (MW)
P_{rf} = 1.5 MW
P_e
(Expt.)
P_e
(PICES)
0.0 0.2 0.4 0.6 0.8 1.0
NORMALIZED RADIUS (r/a)

Figure 7

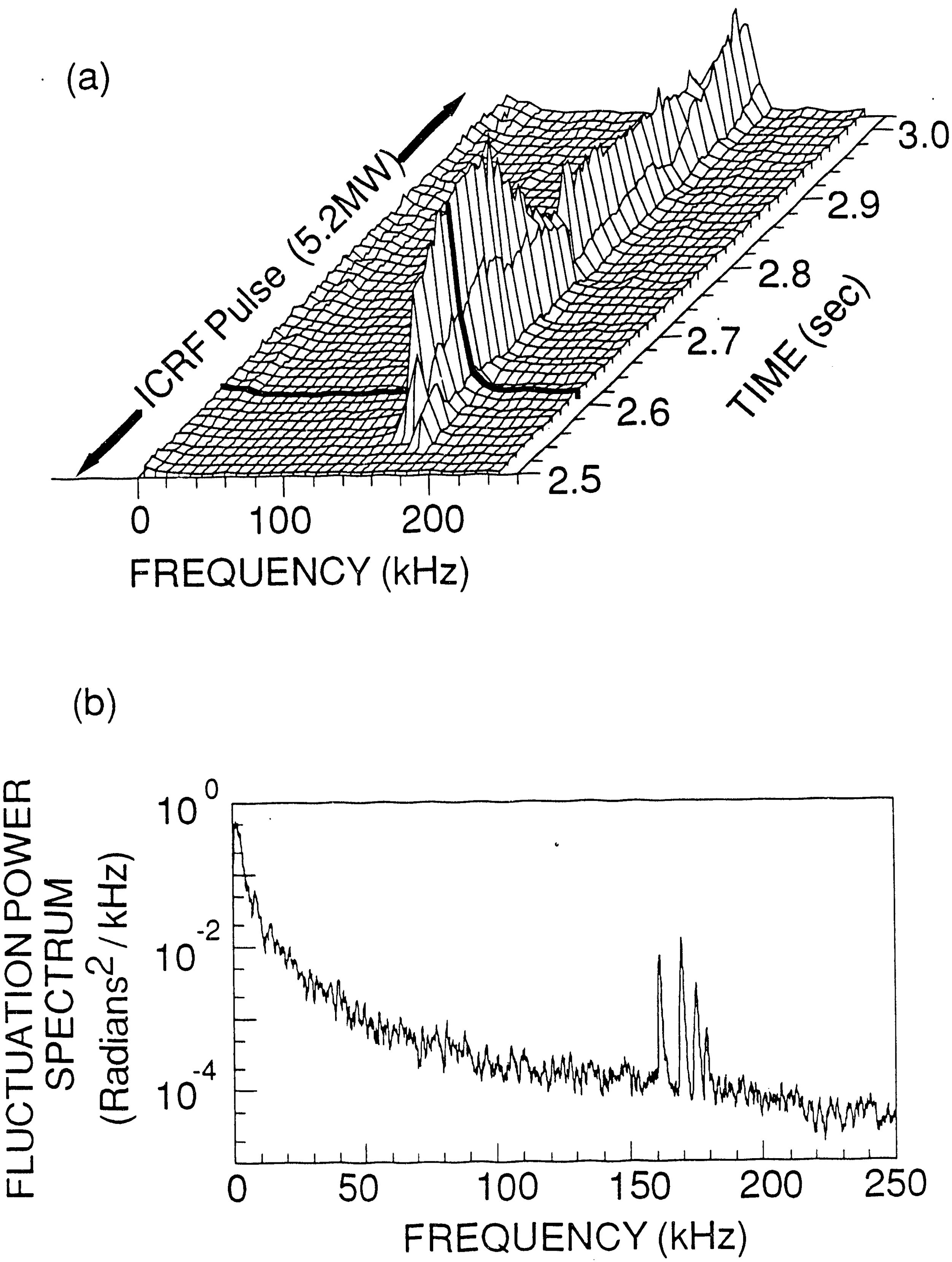
(a)
ICRF Pulse (5.2MW)
3.0
2.9
2.8
2.7
2.6
2.5
TIME (sec)
0
100
200
FREQUENCY (kHz)
(b)
FLUCTUATION POWER SPECTRUM
(Radians^2 / kHz)
10^0
10^{-2}
10^{-4}
0
50
100
150
200
250
FREQUENCY (kHz)

Figure 8

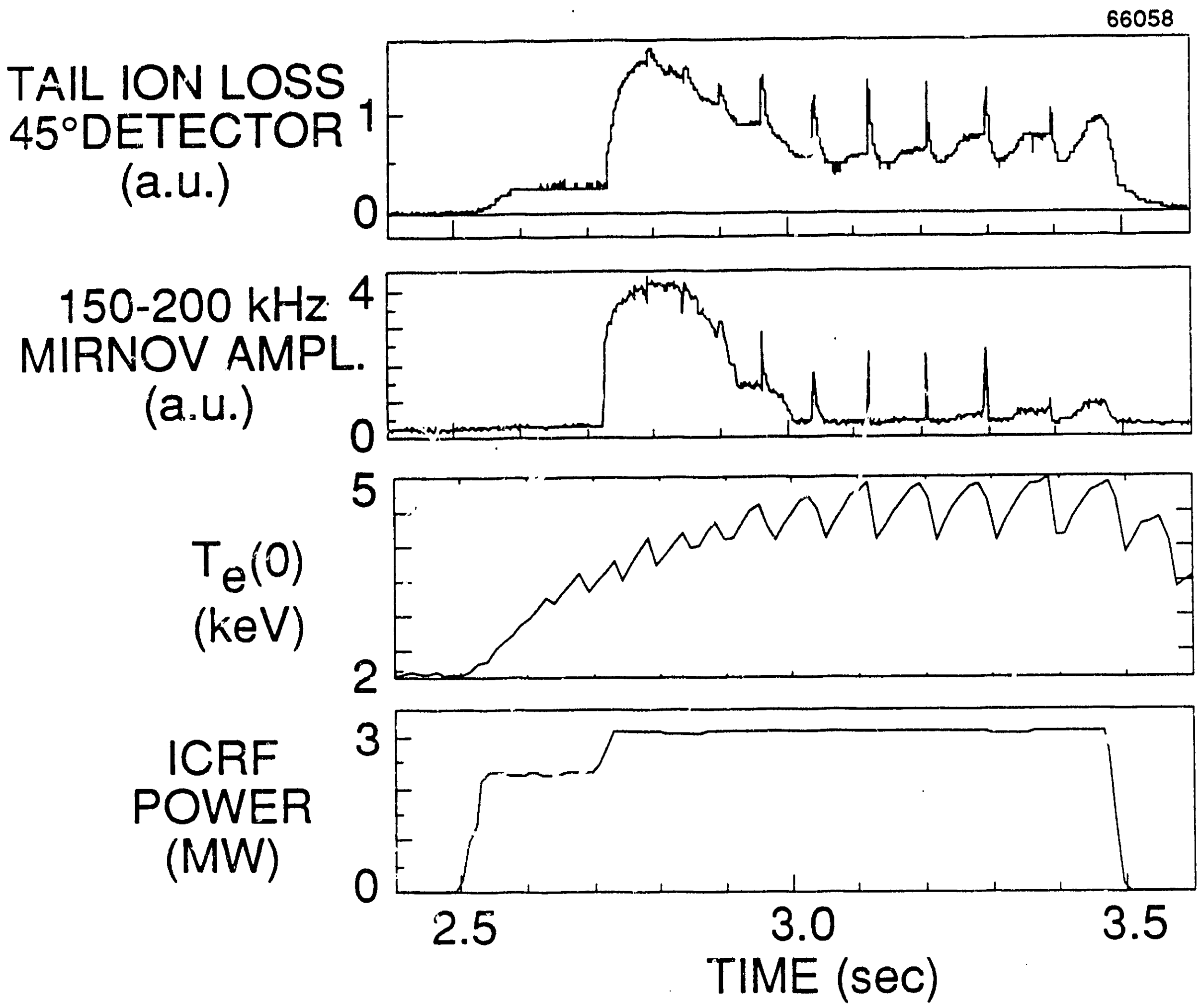
66058
TAIL ION LOSS
45°DETECTOR
(a.u.)
1
0
150-200 kHz
MIRNOV AMPL.
(a.u.)
4
0
5
$T_e(0)$
(keV)
2
ICRF
POWER
(MW)
3
0
2.5
3.0
3.5
TIME (sec)

Figure 9

EXTERNAL DISTRIBUTION IN ADDITION TO UC-420

Dr. F. Paoloni, Univ. of Wollongong, AUSTRALIA
Prof. M.H. Brennan, Univ. of Sydney, AUSTRALIA
Plasma Research Lab., Australian Nat. Univ., AUSTRALIA
Prof. I.R. Jones, Flinders Univ, AUSTRALIA
Prof. F. Cap, Inst. for Theoretical Physics, AUSTRIA
Prof. M. Heindler, Institut für Theoretische Physik, AUSTRIA
Prof. M. Goossens, Astronomisch Instituut, BELGIUM
Ecole Royale Militaire, Lab. de Phy. Plasmas, BELGIUM
Commission-European, DG. XII-Fusion Prog., BELGIUM
Prof. R. Boucíqué, Rijksuniversiteit Gent, BELGIUM
Dr. P.H. Sakanaka, Instituto Fisica, BRAZIL
Instituto Nacional De Pesquisas Espaciais-INPE, BRAZIL
Documents Office, Atomic Energy of Canada Ltd., CANADA
Dr. M.P. Bachynski, MPB Technologies, Inc., CANADA
Dr. H.M. Skarsgard, Univ. of Saskatchewan, CANADA
Prof. J. Teichmann, Univ. of Montreal, CANADA
Prof. S.R. Sreenivasan, Univ. of Calgary, CANADA
Prof. T.W. Johnston, INRS-Energie, CANADA
Dr. R. Bolton, Centre canadien de fusion magnétique, CANADA
Dr. C.R. James,, Univ. of Alberta, CANADA
Dr. P. Lukác, Komenského Universzita, CZECHO-SLOVAKIA
The Librarian, Culham Laboratory, ENGLAND
Library, R61, Rutherford Appleton Laboratory, ENGLAND
Mrs. S.A. Hutchinson, JET Library, ENGLAND
Dr. S.C. Sharma, Univ. of South Pacific, FIJI ISLANDS
P. Mähönen, Univ. of Helsinki, FINLAND
Prof. M.N. Bussac, Ecole Polytechnique,, FRANCE
C. Mouttet, Lab. de Physique des Milieux Ionisés, FRANCE
J. Radet, CEN/CADARACHE - Bat 506, FRANCE
Prof. E. Economou, Univ. of Crete, GREECE
Ms. C. Rinni, Univ. of Ioannina, GREECE
Dr. T. Mual, Academy Bibliographic Ser., HONG KONG
Preprint Library, Hungarian Academy of Sci., HUNGARY
Dr. B. DasGupta, Saha Inst. of Nuclear Physics, INDIA
Dr. P. Kaw, Inst. for Plasma Research, INDIA
Dr. P. Rosenau, Israel Inst. of Technology, ISRAEL
Librarian, International Center for Theo Physics, ITALY
Miss C. De Palo, Associazione EURATOM-ENEA , ITALY
Dr. G. Grosso, Istituto di Fisica del Plasma, ITALY
Prof. G. Rostangni, Istituto Gas Ionizzati Del Cnr, ITALY
Dr. H. Yamato, Toshiba Res & Devel Center, JAPAN
Prof. I. Kawakami, Hiroshima Univ., JAPAN
Prof. K. Nishikawa, Hiroshima Univ., JAPAN
Director, Japan Atomic Energy Research Inst., JAPAN
Prof. S. Itoh, Kyushu Univ., JAPAN
Research Info. Ctr., National Instit. for Fusion Science, JAPAN
Prof. S. Tanaka, Kyoto Univ., JAPAN
Library, Kyoto Univ., JAPAN
Prof. N. Inoue, Univ. of Tokyo, JAPAN
Secretary, Plasma Section, Electrotechnical Lab., JAPAN
S. Mori, Technical Advisor, JAERI, JAPAN
Dr. O. Mitarai, Kumamoto Inst. of Technology, JAPAN
J. Hyeon-Sook, Korea Atomic Energy Research Inst., KOREA
D.I. Choi, The Korea Adv. Inst. of Sci. & Tech., KOREA
Prof. B.S. Liley, Univ. of Waikato, NEW ZEALAND
Inst of Physics, Chinese Acad Sci PEOPLE'S REP. OF CHINA
Library, Inst. of Plasma Physics, PEOPLE'S REP. OF CHINA
Tsinghua Univ. Library, PEOPLE'S REPUBLIC OF CHINA
Z. Li, S.W. Inst Physics, PEOPLE'S REPUBLIC OF CHINA
Prof. J.A.C. Cabral, Instituto Superior Tecnico, PORTUGAL
Dr. O. Petrus, AL I CUZA Univ., ROMANIA
Dr. J. de Villiers, Fusion Studies, AEC, S. AFRICA
Prof. M.A. Hellberg, Univ. of Natal, S. AFRICA
Prof. D.E. Kim, Pohang Inst. of Sci. & Tech., SO. KOREA
Prof. C.I.E.M.A.T, Fusion Division Library, SPAIN
Dr. L. Stenflo, Univ. of UMEA, SWEDEN
Library, Royal Inst. of Technology, SWEDEN
Prof. H. Wilhelmson, Chalmers Univ. of Tech., SWEDEN
Centre Phys. Des Plasmas, Ecole Polytech, SWITZERLAND
Bibliotheek, Inst. Voor Plasma-Fysica, THE NETHERLANDS
Asst. Prof. Dr. S. Cakir, Middle East Tech. Univ., TURKEY
Dr. V.A. Glukhikh, Sci. Res. Inst. Electrophys.I Apparatus, USSR
Dr. D.D. Ryutov, Siberian Branch of Academy of Sci., USSR
Dr. G.A. Eliseev, I.V. Kurchatov Inst., USSR
Librarian, The Ukr.SSR Academy of Sciences, USSR
Dr. L.M. Kovrizhnykh, Inst. of General Physics, USSR
Kernforschungsanlage GmbH, Zentralbibliothek, W. GERMANY
Bibliothek, Inst. Für Plasmaforschung, W. GERMANY
Prof. K. Schindler, Ruhr-Universität Bochum, W. GERMANY
Dr. F. Wagner, (ASDEX), Max-Planck-Institut, W. GERMANY
Librarian, Max-Planck-Institut, W. GERMANY
Prof. R.K. Janev, Inst. of Physics, YUGOSLAVIA

DATE
FILMED
9/10/93

END